NRL Report 6870

Corrosion-Fatigue Crack Propagation Studies of Some New High-Strength Structural Steels

T. W. Crooker and E. A. Lange

Strength of Metals Branch
Metallurgy Division

April 3, 1969

NAVAL RESEARCH LABORATORY
Washington, D.C.

CONTENTS

ABSTRACT

Fatigue crack propagation studies were conducted on three new high-strength structural steels: 9Ni-4Co-0.20C, quenched and tempered; 10Ni-2Cr-1Mo-8Co, dual strengthened; and 13Cr-8Ni-2Mo, precipitation-hardened stainless. The yield strengths of these steels ranged from 176 to 193 ksi. Notched cantilever-bend specimens of each steel were cycled zero-to-tension in two environments — room air and 3.5% NaCl salt water. Fatigue crack growth rates were measured experimentally and correlated with the crack tip stress-intensity factor range. The results indicate that these new steels possess greater resistance to fatigue crack propagation and less sensitivity to environment than previously studied steels of comparable strength.

PROBLEM STATUS

This report covers one phase of the problem; work is continuing.

AUTHORIZATION

NRL Problem M01-25
Projects SF 51-541-003-12383 and
RR 007-01-46-5432

Manuscript submitted December 9, 1968.

CORROSION-FATIGUE CRACK PROPAGATION STUDIES OF SOME NEW HIGH-STRENGTH STRUCTURAL STEELS

NOMENCLATURE

a	flaw depth (machined notch plus fatigue crack)
B	specimen thickness (nominal thickness not including side grooves)
C	material constant
2c	length of embedded surface crack
D	specimen width
da/dN	crack extension per cycle of load (fatigue crack growth rate)
K	fracture mechanics stress-intensity factor
ΔK	stress-intensity factor range (maximum K minus minimum K)
K_{max}	maximum stress-intensity factor
K_{Ic}	critical stress-intensity factor for initial crack instability in plane strain (plane strain fracture toughness)
K_{Iscc}	threshold stress intensity factor for stress-corrosion cracking in plane strain
m	numerical exponent
R	load ratio (minimum load:maximum load)
r_y	crack tip plastic zone size
SEN	single edge notched
σ_{ys}	0.2%-yield-strength stress
$\Delta\sigma$	cyclic stress range

INTRODUCTION

The evolution of high-strength structural steels has essentially proceeded in three phases. Initial efforts involved quenched-and-tempered steels with sufficient carbon content to produce high strength levels and sufficient alloy content for through hardenability in relatively thick sections. Structural experience with these early high-strength steels was plagued by numerous dramatic failures, due to brittle fracture, fatigue, or stress corrosion. The second phase of development involved efforts to improve fracture

toughness. New steels, such as maraging steels with minimum carbon content, were introduced, and processing techniques were improved through procedures such as vacuum melting. However, many of these newer steels remained highly susceptible to stress-corrosion cracking. The third and current phase is aimed at the development of high-strength, high-toughness steels that combine the best metallurgical features of the previous alloy systems and are also more resistant to stress-corrosion cracking.

This report concerns recent studies of corrosion-fatigue crack propagation in three new high-strength structural steels: 9Ni-4Co-0.20C, quenched and tempered; 10Ni-2Cr-1Mo-8Co, dual strengthened; and 13Cr-8Ni-2Mo precipitation-hardened stainless. The purpose of this study was to establish the fatigue characteristics of these new steels on a comparative basis with previous work on older steels (1,2).

MATERIALS AND PROCEDURES

The chemical, metallurgical, and mechanical descriptions of the steels under investigation are summarized in Tables 1 through 3.

Table 1
Chemical Composition

Alloy	Chemical Composition (wt-%)										
	C	Mn	P	S	Si	Ni	Cr	Mo	Co	V	Al
9Ni-4Co-0.20C*	0.17-0.23	0.20-0.40	0.010 max.	0.010 max.	0.10 max.	8.50-9.50	0.65-0.85	0.90-1.10	4.25-4.75	0.06-0.10	—
10Ni-2Cr-1Mo-8Co	0.12	0.094	0.003	0.007	0.030	9.88	2.09	1.05	7.96	—	0.002
13Cr-8Ni-2Mo	0.042	0.02	0.003	0.004	0.02	8.07	12.58	2.06	—	—	1.11

*Manufacturer's specifications.

Table 2
Processing and Heat Treatment

Alloy	Remarks
9Ni-4Co-0.20C	Consumable-electrode vacuum melted Highly cross-rolled to 1-in. plate Mill quenched and tempered
10Ni-2Cr-1Mo-8Co	Vacuum-induction melted and vacuum arc remelted Rolled to 1-in. plate Mill heat treated: austenitized at 1500°F for 1 hour, water quenched, aged at 950°F for 7 hours, water quenched
13Cr-8Ni-2Mo	Vacuum-induction melted and vacuum-electrode remelted Rolled to 1-in. plate Mill solution annealed and NRL aged at 1050°F for 4 hours

Table 3
Tensile and Impact Properties

Alloy	Fracture Path Orientation*	0.505-In.-Diam Tensile Test Data				C_v Energy at 30°F (ft-lb)
		0.2% YS (ksi)	UTS (ksi)	Elong. in 2 In. (%)	R.A. (%)	
9Ni-4Co-0.20C	WR	183.0	201.3	17.8	66.0	60
	RW	—	—	—	—	—
10Ni-2Cr-1Mo-8Co	WR	193.3	208.0	16.5	69.5	68
	RW	—	—	—	—	80
13Cr-8Ni-2Mo	WR	176.1	182.5	18.5	69.8	51
	RW	176.5	183.0	17.7	68.5	56

*RW = transverse; WR = Longitudinal as defined in Ref. 3.

Fatigue crack propagation characteristics were investigated using single-edge-notched (SEN) specimens cycled under constant load, zero-to-tension, in cantilever bending at 5 cpm. A detailed drawing of the fatigue specimen is shown in Fig. 1. The test section has nominal dimensions of 2.5 in. wide and 0.5 in. thick. The net thickness is reduced to 0.45 in. by side grooving, which acts to suppress shear lip formation and promote a straight crack front. The edge notch is nominally 0.5 in. deep, and fatigue crack propagation is allowed to extend the flaw to a maximum total depth of 1.5 in. (a/D = 0.6). Measurements of fatigue crack length are performed by a slide-mounted optical micrometer focused on the root surface of one side groove.

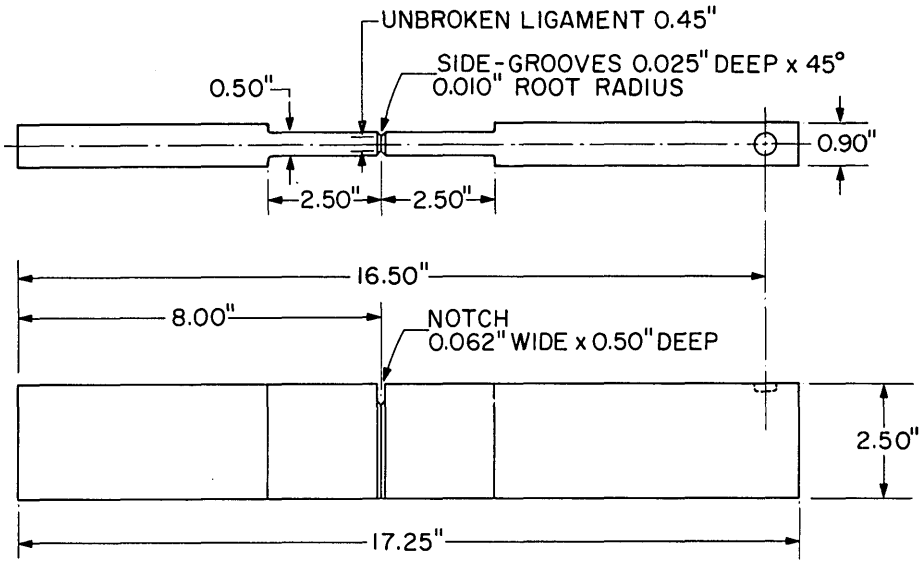

Fig. 1 - Details of the fatigue specimen

As the crack propagates through the test section under constant load, the stress-intensity factor range increases, thus producing a range of crack growth rates for study. Specimens were cycled until the maximum flaw size of 1.5 in. was grown, unless gross yielding occurred first. Continuous moment arm deflection measurements, displayed on a strip recorder, indicated the onset of gross yielding. None of the specimens employed in this investigation failed by brittle, instability fracture. Stress-intensity factor values were computed using Kies's equation (4).

RESULTS AND DISCUSSION

The fatigue data presented in this report are expressed in terms of the crack growth rate da/dN as a function of the stress-intensity factor range ΔK. This method of data presentation is preferred, because it is a generalized means of expressing fatigue crack propagation data. A growth rate analysis based on stress-intensity can be translated from laboratory specimens to structures, since it can be restated in terms of specific stress levels and flaw sizes.

Efforts to apply linear elastic fracture mechanics to fatigue crack propagation were initiated by Paris and Erdogan (5). A significant amount of evidence now exists in support of many of their early conclusions (6). In generalized form, fatigue crack growth rates can be expressed as a function of the stress-intensity factor range:

$$da/dN = C(\Delta K)^m . \tag{1}$$

The values of C and m vary with the material and the load ratio (6-8). For steels, m can vary from values slightly greater than 2 to values exceeding 6 (1,2,9-14). For high-strength, high-toughness steels cycled zero-to-tension (R = 0), such as those studied in this investigation, m has been found to vary from approximately 2 to 4. Values of m significantly greater than 4 occur principally in low-toughness steels (10,13) or at higher ΔK levels approaching instability (10,11,15).

There is little evidence to suggest that the stress state (i.e., plane stress or plane strain) is a significant variable in fatigue crack propagation (6,16). However, plane strain restraint at the crack tip is a necessary condition for stress-corrosion cracking to occur (17); therefore, some consideration of the stress state should be included in corrosion-fatigue studies of materials, such as high-strength steels, which are sensitive to stress-corrosion cracking.

The degree of restraint existing at the crack tip is measured by the relative size of the plastic zone in relation to the dimensions of the test specimen. For the specimen employed in this investigation, the critical specimen dimension is the thickness. Figure 2 shows the plastic-zone-size-to-thickness ratio versus ΔK for the specimen and materials employed in this investigation. Two curves are shown; the upper curve refers to the plane stress plastic zone for monotonic loading,

$$r_y = \frac{1}{2\pi}(\Delta K/\sigma_{ys})^2 , \tag{2}$$

and the lower curve refers to the plastic zone size in fatigue, as estimated by Paris to be 1/4 as great (6):

$$r_y = \frac{1}{8\pi}(\Delta K/\sigma_{ys})^2 . \tag{3}$$

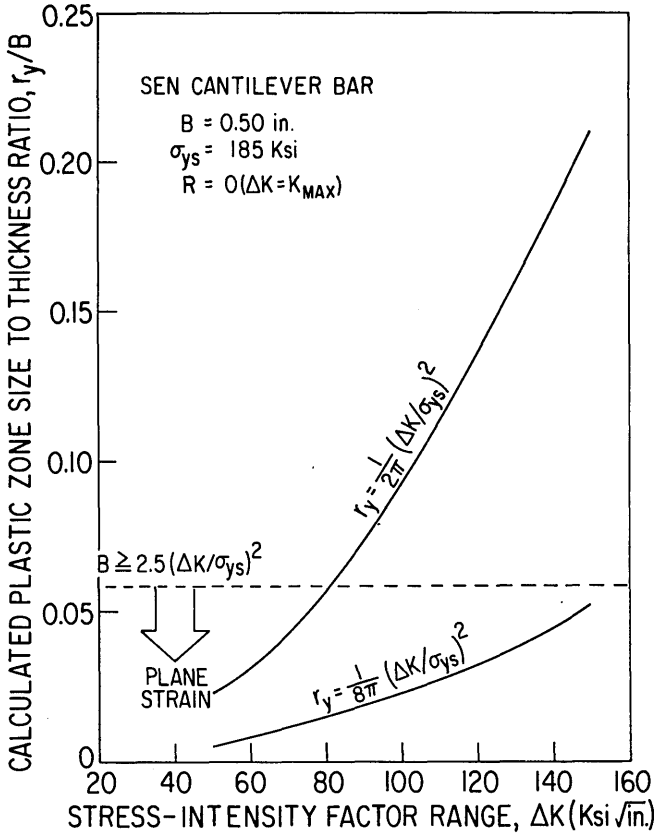

Fig. 2 - Calculated plastic-zone-size-to-thickness ratio as a function of stress-intensity factor range for a 0.50-in.-thick specimen of a 185-yield-strength material. The upper curve refers to plane stress monotonic loading, and the lower curve refers to fatigue loading. The limiting condition for plane strain, as defined by the ASTM Committee E-24, is indicated by the dashed line.

In addition, on Fig. 2 the upper limit for plane strain conditions as established by ASTM Committee E-24 for fracture toughness testing (18),

$$B \geq 2.5\,(\Delta K/\sigma_{ys})^2, \tag{4}$$

is indicated by the dashed line. Based on Eq. 3 for plastic zone sizes in fatigue, it would appear that all of the data presented in this report were obtained under plane strain conditions. The ΔK values reported are not corrected for plasticity, because the corrections involved using Eq. 3 are very small. All of the higher ΔK values reported were obtained from relatively deep flaws ($a/D = 0.4 \rightarrow 0.6$), where r_y was very small in proportion to a.

The fatigue results are shown in Figs. 3 through 5. These are log-linear plots of da/dN (log scale) versus ΔK (linear scale). The open symbols denote data from air environment tests, and the closed symbols denote data from saltwater environment tests. Log-linear coordinates were chosen, rather than the more commonly used log-log

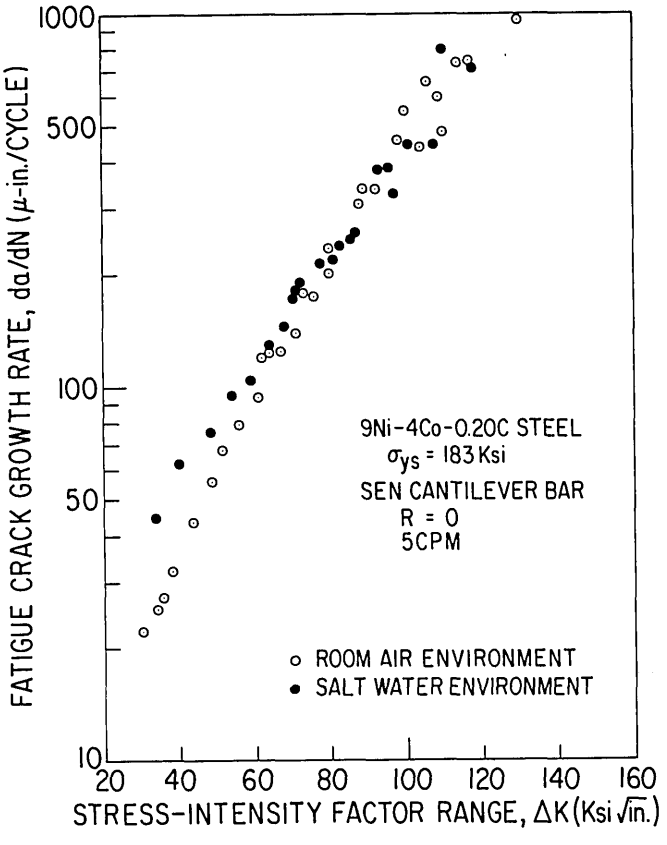

Fig. 3 - Log-linear plot of fatigue crack growth rate data as a function of stress-intensity factor range for 9Ni-4Co-0.20C steel in air and saltwater environments.

coordinates, because the authors feel that the environmental effects were more clearly illustrated.

Several observations are apparent from the data presented on Figs. 3 through 5. First, these steels are not highly fatigue sensitive to the saltwater environment. Looking back at high-strength, quenched-and-tempered steels of the 4340 type studied just a few years ago (19,20), considerable progress has been made in improving the corrosion-fatigue crack propagation resistance of high-strength steels. Fatigue crack growth rates in 4340-type steels can increase by more than a factor of 10, due to the presence of a salt water environment. In contrast, the maximum environmental effects observed in the new steels studied in this investigation involved fatigue crack growth rates which were increased by factors of 2 to 3. Second, in each case the greatest environmental effects occurred at low ΔK levels, near 40 ksi $\sqrt{in.}$ Environmental effects decreased as ΔK increased above this value; in each case, data for the two environments merged at higher ΔK values. This pattern of behavior has been observed previously in recent studies of similar steels (1,2). There may be some significance in the fact that convergence of the air and saltwater environment fatigue data occurs, in each case, near the upper stress-intensity limit for plane strain in monotonic loading, as shown in Fig. 2. A further investigation of this phenomenon, using thicker specimens with a higher limiting plane strain stress-intensity, is being undertaken.

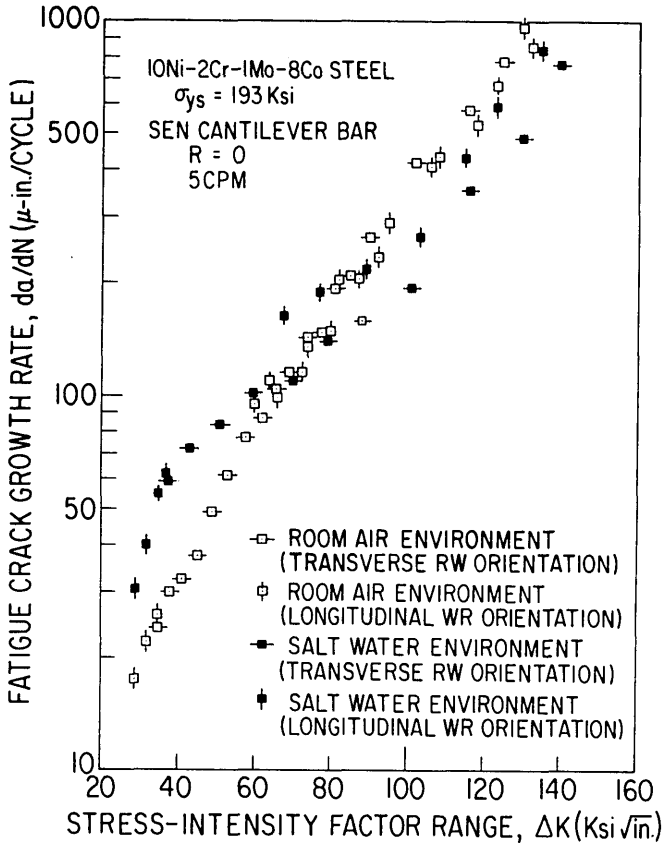

Fig. 4 - Log-linear plot of fatigue crack growth rate data for 10Ni-2Cr-1Mo-8Co steel. Note that specimens were tested in two fracture path orientations — longitudinal and transverse.

Plane strain fracture toughness K_{Ic} and stress-corrosion cracking K_{Iscc} tests have not been performed on these specific samples of each material. However, typical values for these alloys (21-23) place the K_{Ic} levels well above the upper limit of ΔK values encountered in this fatigue research program and the K_{Iscc} levels at or near the upper limit. Hence, the maximum stress-intensity value used to propagate the crack by a fatigue growth mechanism was less than the critical stress-intensity values below which stress-corrosion cracking or plane strain fracture cannot conceivably occur. It is significant that the greatest environmental effects observed under cyclic loading occurred far below the stress-intensity levels required for stress-corrosion cracking under a static load. This strongly suggests that environmentally-assisted fatigue should be viewed as a separate phenomenon from stress-corrosion cracking. From a practical point of view, these results suggest that the most important effect than an aggressive aqueous environment may have on the structural application of these alloys is to accelerate the growth of small defects, thus possibly eliminating an important early phase in the fatigue life of a structure.

Among the steels studied, only the 10Ni alloy was tested in two fracture path orientations — longitudinal (WR) and transverse (RW). Each of the other alloys were tested only in the WR orientation. Figure 4 indicates there were some effects due to anisotropy in the saltwater environment, but none were apparent in the air environment. This

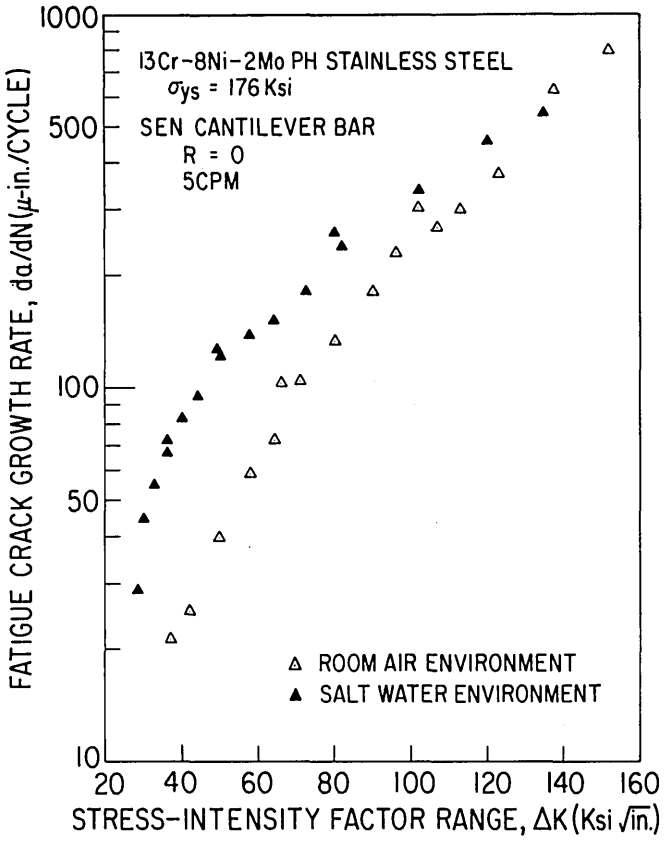

Fig. 5 - Log-linear plot of fatigue crack growth rate data for 13Cr-8Ni-2Mo PH stainless steel

agrees with previous studies on high-strength steels (20), although significant anisotropy effects in steels fatigued in an air environment have been observed in forged steels (9,14).

The 10Ni data shown in Fig. 4 indicate that at higher ΔK levels crack growth rates were lower in salt water than in air. This phenomenon is considered by the authors to be indicative of an absence of environmental sensitivity but is not an indication of improved fatigue performance in salt water. A possible explanation may lie in a favorable degree of crack blunting caused by the corrosive environment under the particular conditions of the test.

On a comparative basis, the 9Ni and 10Ni alloys studied appear to be nearly equal in corrosion-fatigue performance. The precipitation-hardened stainless alloy exhibited the greatest sensitivity to environment. However, this alloy possesses fatigue properties nearly identical to a 12Ni 180-grade maraging steel previously studied (1,2,24). The results of this previous study on three steels clearly indicated the 12Ni alloy to be superior among that initial group. Thus, it would appear that improved corrosion-fatigue crack propagation characteristics are resulting from efforts to improve fracture toughness and stress-corrosion cracking resistance in 180-ksi yield-strength steels.

A summary of the air environment fatigue data for the three steels studied is shown plotted on log-log coordinates in Fig. 6. The data for the 9Ni and 10Ni alloys follow a

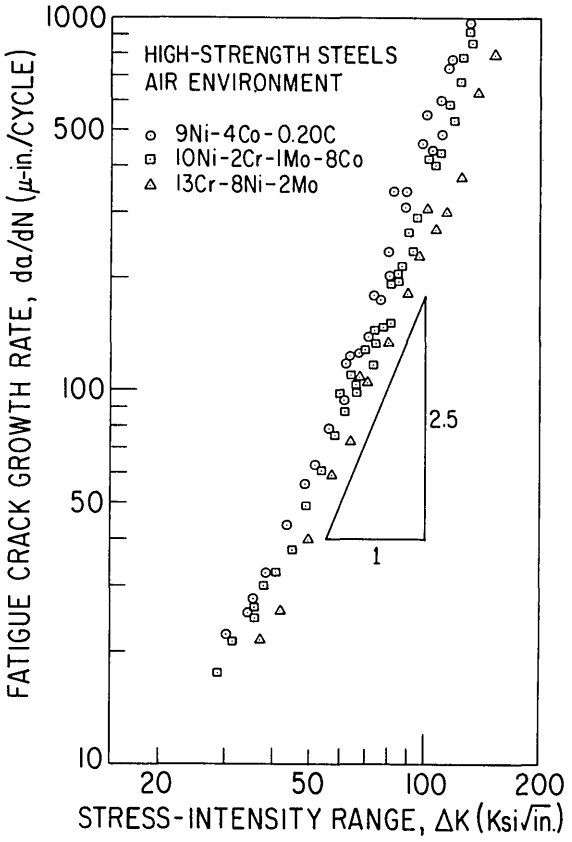

Fig. 6 - Log-log summary plot of air environment fatigue crack growth rate data for three steels. A reference slope of 2.5:1 is indicated.

common curve for all practical purposes. The PH stainless alloy tends to be slightly below the other two alloys. A slope of 2.5:1 is shown for reference.

One of the advantages of expressing fatigue crack growth rate data as a function of ΔK is that it can be restated in terms of stress levels and flaw sizes. Figure 7 shows one translation of the fatigue crack growth rates into structural parameters of flaw size and stress level. This example is presented because it improves the visibility of the general fatigue situation and provides a qualitative estimate of potential fatigue failure for the stress levels and flaw sizes that might be encountered in service. The stress level-flaw size relationships for failure by instability fracture in these and similar alloys are given in Ref. 25. Some discussion of stress level-flaw size interpretations of stress-corrosion cracking failure is given in Ref. 22.

Figure 7 is a linear plot of cyclic stress level versus flaw depth showing three contours of constant crack growth rate (ΔK = constant), based on the data summarized in Fig. 6. Contours for da/dN = 10, 100, and 1000 μ-in./cycle are shown and represent slow, medium, and fast growth rates with respect to low-cycle fatigue. The curves apply to a semicircular-shaped surface flaw in a plate loaded axially from zero-to-tension. The fracture mechanics analysis of surface-cracked plates to simulate structural failure situations is discussed in Ref. 26.

The curves shown apply only to the specific conditions described. Aqueous environments, tensile mean loads (tensile residual stresses), or changes in flaw shape ($a/2c < 0.50$) can all act to shift these curves downward and to the left, i.e., to lower stress

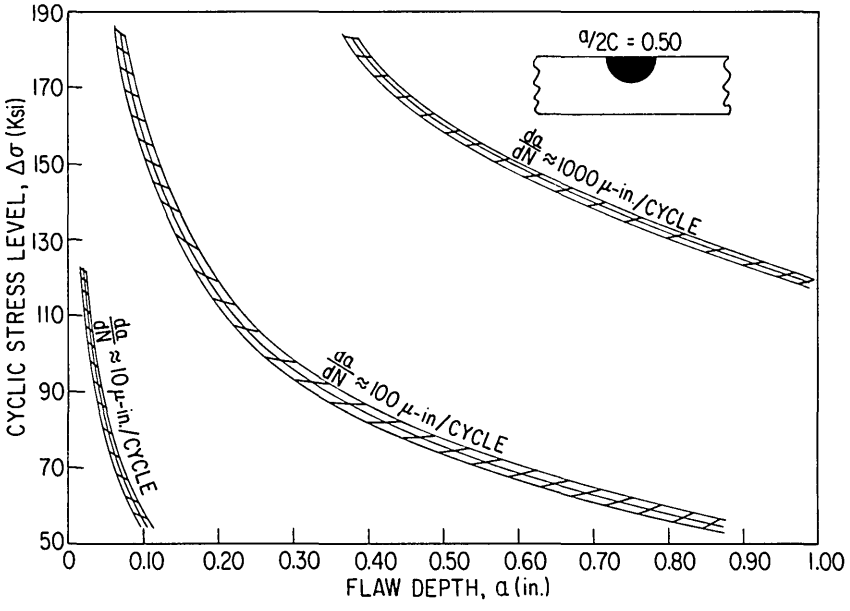

Fig. 7 - Cyclic stress level versus flaw depth relationships showing the locus of constant fatigue crack growth rates (constant ΔK levels). The curves are based on air environment data for the three steels studied and apply to the predicted behavior of a semicircular surface flaw in a plate loaded axially zero-to-tension.

levels and/or smaller flaw sizes. Therefore, it can be seen that, although these steels possess some of the best fatigue resistance presently available, crack growth will occur fairly rapidly at the high stress levels of which these alloys are capable.

CONCLUSIONS

The following conclusions have been reached from this study:

1. The 9Ni-4Co-0.20C and 10Ni-2Cr-1Mo-8Co alloys exhibited less sensitivity to saltwater environment than the 13Cr-8Ni-2Mo PH steel. The two former steels possessed nearly identical fatigue crack propagation characteristics, measured as a function of stress-intensity, in both the ambient air and 3.5% NaCl salt water environments.

2. The 13Cr-8Ni-2Mo precipitation-hardened stainless steel exhibited somewhat greater sensitivity to the saltwater environment than did the other alloys studied. However, the results obtained from this study indicate that these three new steels possess significantly greater resistance to fatigue crack propagation and less sensitivity to environment than previously studied steels of comparable strength.

3. For each steel, the greatest sensitivity to environment occurred at low stress-intensity levels, near 40 ksi $\sqrt{\text{in.}}$, which is far below the stress-intensity threshold level necessary for stress-corrosion cracking to occur. Environmental sensitivity decreased with increasing stress-intensity, and convergence of data from both air and saltwater environments occurred at higher stress-intensity levels in all three steels.

4. The fatigue crack propagation characteristics of all three steels in air were similar, and the data fell along a narrow scatterband described by the relationship $da/dN = C(\Delta K)^{2.5}$.

5. A graphical display of the relationships between flaw size, stress levels, and fatigue crack growth rates indicates that these materials have good resistance to the growth of flaws of readily detectable sizes, even at stress levels approaching yield strength.

ACKNOWLEDGMENTS

The authors acknowledge the work of Mr. R. J. Hicks, who performed the fatigue tests. The authors are also grateful to the Office of Naval Research, the Naval Ship Systems Command, Code 03422, and the Deep Submergence Systems Project, Code 221, for their financial support of this work.

REFERENCES

1. Crooker, T.W., and Lange, E.A., "Fatigue Crack Growth in Three 180-ksi Yield Strength Steels in Air and in Salt Water Environments," NRL Report 6761, Sept. 1968

2. Crooker, T.W., and Lange, E.A., "The Influence of Salt Water on Fatigue Crack Growth in High-Strength Structural Steels," ASTM Symposium on Fatigue, 1968 Fall Meeting, Atlanta, Georgia, Sept. 29-Oct. 4, 1968 (publication pending)

3. ASTM Committee on Fracture Testing of High-Strength Metallic Materials, "The Slow Growth and Rapid Propagation of Cracks," Mater. Res. Std. 1 (No. 5):389 (1961)

4. Kies, J.A., Smith, H.L., Romine, H.E., and Bernstein, H., "Fracture Testing of Weldments," in Fracture Toughness Testing and Its Applications," ASTM STP 381, Philadelphia:American Society for Testing and Materials, p. 328, 1965

5. Paris, P.C., and Erdogan, F., "A Critical Analysis of Crack Propagation Laws," J. Basic Eng., Transactions ASME 8SD:528 (1963)

6. Johnson, H.H., and Paris, P.C., "Sub-Critical Flaw Growth," J. Eng. Fracture Mech. 1 (No. 1):3 (1968)

7. Forman, R.G., Kearney, V.E., and Engle, R.M., "Numerical Analysis of Crack Propagation in Cyclic-Loaded Structures," J. Basic Eng., Transactions ASME 89D (No. 3): 459 (1967)

8. Crooker, T.W., and Lange, E.A., "Fatigue Crack Propagation in a High-Strength Steel Under Constant Cyclic Load With Variable Mean Loads," NRL Report 6805, Nov. 1968

9. Brothers, A.J., and Yukawa, S., "Fatigue Crack Propagation in Low-Alloy Heat-Treated Steels," J. Basic Eng., Transactions of ASME 89D (No. 1):19 (1967)

10. Carman, C.M., and Katlin, J.M., "Low Cycle Fatigue Crack Propagation Characteristics of High Strength Steels," J. Basic Eng., Transactions of ASME 88 (No. 4) (1966)

11. Clark, W.G., Jr., "Subcritical Crack Growth and Its Effect Upon the Fatigue Characteristics of Structural Alloys," J. Eng. Fracture Mech. 1 (No. 2):385 (1968)

12. Rolfe, S.T., U.S. Steel Applied Research Laboratory, private communication

13. Miller, G.A., "The Dependence of Fatigue-Crack Growth Rate on the Stress Intensity Factor and the Mechanical Properties of Some High-Strength Steels," ASM Trans. Quart. 61 (No. 3):442 (1968)

14. Mowbray, D.F., Andrews, W.R., and Brothers, A.J., "Fatigue-Crack Growth-Rate Studies of Low-Alloy Pressure Vessel Steels," J. Eng. Ind. 90B (No. 4):648 (1968)

15. Crooker, T.W., Cooley, L.A., Lange, E.A., and Freed, C.N., "Fatigue Crack Propagation and Plane Strain Fracture Toughness Characteristics of a 9Ni-4Co-0.25C Steel," ASM Trans. Quart. 61 (No. 3):568 (1968)

16. Clark, W.G., Jr., and Trout, H.E., "Influence of Temperature and Section Size on Fatigue Crack Growth Behavior in Ni-Mo-V Alloy Steel," National Symposium on Fracture Mechanics, Lehigh University, Bethlehem, Pennsylvania, June 17-19, 1968

17. Brown, B.F., "A New Stress-Corrosion Cracking Test for High-Strength Alloys," Mater. Res. Std. 6 (No. 3):129 (1966)

18. Brown, W.F., Jr., and Srawley, J.E., "Plane Strain Crack Toughness Testing of High-Strength Metallic Materials," ASTM STP 410, Philadelphia:American Society for Testing and Materials, 1966

19. Crooker, T.W., and Lange, E.A., "Low Cycle Fatigue Crack Propagation Resistance of Materials for Large Welded Structures," in "Fatigue Crack Propagation," ASTM STP 415, Philadelphia:American Society for Testing and Materials, p. 94, 1967

20. Crooker, T.W., and Lange, E.A., "Corrosion-Fatigue Crack Propagation in Modern High-Performance Structural Steels," ASM Trans. Quart. 60 (No. 2):198 (1967)

21. Novak, S.R., and Rolfe, S.T., "K_{Iscc} Tests of HY-180/210 Steels and Weld Metals," U.S. Steel Applied Research Laboratory Technical Report, Aug. 1, 1967

22. Sandoz, G., "The Susceptibility to Slow Crack Growth of Some High Strength Steels in Salt Water," ASTM Symposium on Stress Corrosion and Corrosion Principles, 1968 Fall Meeting, Atlanta, Georgia, Sept. 29-Oct. 4, 1968

23. Clark, W.G., Jr., and Wessel, E.T., "Influence of the Marine Environment on the Fracture Behavior of HP 9-4-25 and HP 9-4-20 Alloy Steels," ASTM Symposium on Materials and the Deep Sea Environment, 1968 Annual Meeting, San Francisco, California, June 24-28, 1968

24. Crooker, T.W., and Lange, E.A., "Fatigue Crack Growth in High-Strength Structural Steels," Report of NRL Progress, p. 25, July 1968

25. Pellini, W.S., "Advances in Fracture Toughness Characterization Procedures in Quantitative Interpretations to Fracture-Safe Design for Structural Steels," Welding Research Council Bulletin 130, May 1968

26. Tiffany, C.F., and Masters, J.N., "Applied Fracture Mechanics," in "Fracture Toughness Testing and Its Applications," ASTM STP 381, Philadelphia:American Society for Testing and Materials, p. 249, 1965

Security Classification

DOCUMENT CONTROL DATA - R & D

(Security classification of title, body of abstract and indexing annotation must be entered when the overall report is classified)

1. ORIGINATING ACTIVITY (Corporate author)	2a. REPORT SECURITY CLASSIFICATION
Naval Research Laboratory Washington, D.C. 20390	Unclassified
	2b. GROUP

3. REPORT TITLE

CORROSION-FATIGUE CRACK PROPAGATION STUDIES OF SOME NEW HIGH-STRENGTH STRUCTURAL STEELS

4. DESCRIPTIVE NOTES *(Type of report and inclusive dates)*

Interim report; work is continuing.

5. AUTHOR(S) *(First name, middle initial, last name)*

T. W. Crooker and E. A. Lange

6. REPORT DATE	7a. TOTAL NO. OF PAGES	7b. NO. OF REFS
April 3, 1969	18	26

8a. CONTRACT OR GRANT NO.	9a. ORIGINATOR'S REPORT NUMBER(S)
NRL Problem M01-25	
b. PROJECT NO. SF 51-541-003-12383 RR 007-01-46-5432	NRL Report 6870
c.	9b. OTHER REPORT NO(S) *(Any other numbers that may be assigned this report)*
d.	

10. DISTRIBUTION STATEMENT

This document has been approved for public release and sale; its distribution is unlimited.

11. SUPPLEMENTARY NOTES	12. SPONSORING MILITARY ACTIVITY
	Department of the Navy (Naval Ship Systems Command and Office of Naval Research), Washington, D.C. 20360

13. ABSTRACT

Fatigue crack propagation studies were conducted on three new high-strength structural steels: 9Ni-4Co-0.20C, quenched and tempered; 10Ni-2Cr-1Mo-8Co, dual strengthened; and 13Cr-8Ni-2Mo, precipitation-hardened stainless. The yield strengths of these steels ranged from 176 to 193 ksi. Notched cantilever-bend specimens of each steel were cycled zero-to-tension in two environments — room air and 3.5% NaCl salt water. Fatigue crack growth rates were measured experimentally and correlated with the crack tip stress-intensity factor range. The results indicate that these new steels possess greater resistance to fatigue crack propagation and less sensitivity to environment than previously studied steels of comparable strength.

DD FORM 1 NOV 65 1473 (PAGE 1)

S/N 0101-807-6801

Security Classification

14. KEY WORDS	LINK A		LINK B		LINK C	
	ROLE	WT	ROLE	WT	ROLE	WT
Fatigue crack propagation High-strength structural steels Corrosion fatigue						